Nonlinear Model Predictive Control of a Class of Continuum Robots Using Kinematic and Dynamic Models

Ammar Amouri

Assistant Professor, HDR
Department of Mechanical Engineering
Frères Mentouri Constantine 1 University
Algeria

Abdelhakim Cherfia

Assistant Professor, HDR
Department of Mechanical Engineering
Frères Mentouri Constantine 1 University
Algeria

Halim Merabti

Senior Researcher
Research Center in Industrial Technologies
CRTI, P. O. Box 64, Cheraga 16014 Algiers
Algeria

Yazid Laib Dit Leksir

Assistant Professor, HDR
Department of Mechanical Engineering
University of L'Arbi Ben M'hidi, Oum el
Bouaghi
Algeria

Controlling continuum robots with precision is particularly a challenging task due to the complexity of their mathematical models and inaccuracies in modeling approaches. Therefore, most advanced control schemes have shown poor performances, especially in trajectory tracking accuracy. This paper presents a proposed Nonlinear Model Predictive Control (NMPC) scheme to solve the trajectory tracking of a class of continuum robots, namely Cable-Driven Continuum Robot (CDCR). However, since NMPC schemes are often limited by the computational burden associated with the optimization algorithms to be solved at each sampling time, the Particle Swarm Optimization (PSO) algorithm is used to solve the arising optimization problem NMPC, thanks to its simplicity and fast convergence. The proposed NMPC-PSO scheme is applied to the developed kinematic and dynamic models of the considered CDCR. Based on the kinematic and dynamic model, the two proposed controllers have been validated against numerical simulations of two-dimensional CDCR with two bending sections for set-point stabilization and point-to-point trajectory tracking. For both controllers, the performance of tracking accuracy and computation time is analyzed and compared. Moreover, the obtained simulation results are compared to the available literature works. In view of the results obtained on the considered CDCR, the proposed NMPC-PSO scheme can track in real-time the desired trajectory with high accuracy and much less execution time than other advanced control schemes, which makes it an alternative for real-time applications.

.

Keywords: *Continuum robot, cable-driven continuum robot, nonlinear model predictive control, particle swarm optimization, trajectory tracking.*

1. INTRODUCTION

In recent years, the field of continuum robots, whether theoretical research or practical applications, has received significant attention from the robotic community due to the continuum robots' characteristics such as high flexibility, compliance, and, more importantly, their safe interaction. Uniquely, these robots can be of a hard or a soft structure [1, 2], i.e., they have no joints and no rigid parts in their bodies, allowing them to adapt their shape to pick up a range of objects and provide skilled positioning even in restricted environ–ments, mimicking the movement of some animals such as the elephant's trunk, snake's body, and octopus' tentacles. Currently, numerous examples of continuum robots have been built, including the concentric tube continuum robot [3], the tendon-driven continuum robot (TDCR) [4], the pneumatic continuum robot [5], and the cable-driven continuum robot (CDCR) [6] which is under consideration in the present paper.

Continuum robots' modeling is a challenging task. Hence, kinematic models that define the relationship between the robot's configuration and the operational variables must be established for a successful kinematic motion and derivation of the dynamic model. Based on some hypotheses and simplifications, kinematic models of continuum robots are solved. Undoubtedly, the most commonly used approach is the Constant Curvature Kinematic Approach (CCKA) which is successfully applied to different model types of continuum robots [3-10], thanks to its simplicity [7]. In contrast to kinematic modeling, continuum robots' dynamic modeling remains a challenging task due to its complexity and modeling inaccuracies. Despite this, many researchers have made great efforts to study the dynamic behavior of different types of continuum robots using other methods and theories such as the Lagrangian method [5-10], Kine's approach [11-12], Cosserat rod theory [13-14] and Hamilton principle [15-16]. Contrastingly, some researchers have been using a discrete Cosserat app–roach to derive the dynamics of multisection soft mani–pulators [17]. Needless to say, previous works have provided valuable enlightenment in dynamic modeling for continuum robots. A secondary contribution of this paper is the calculation of the kinematic and dynamic models of a planar multi-bending-section CDCR that will be used in the design of the controllers in question.

Controlling a robotic system can be done according to the kinematic or dynamic models. However, according to the literature review, the continuum robot

control problem has been widely investigated using a variety of controllers like the Proportional-Integrated-Derivative (PID) controller and its variants, adaptive control schemes, fuzzy logic controller, model predic–tive control, and others. In terms of kinematic control versus dynamic control, it is obvious that it is commonly employed because it is relatively simple and easier to implement. In contrast, the nonlinear dynamic behavior of continuum robots and the lack of an effi–cient dynamic model make the implementation of its control difficult.

Regarding conventional control schemes, the Pro–portional-Integrated-Derivative controller [6] and a Proportional-Derivative controller [18] were used to ensure the trajectory tracking of a class of continuum robots in a fixed orientation and a planar continuous soft robot, namely vine robot, respectively, both joined with the dynamic model. However, these techniques have limitations, especially when the robot has complexity and uncertainty in the model. Therefore, intelligent control techniques can be considered promising alternatives.

Regarding advanced control techniques or intelligent control techniques, various schemes have been proposed to improve the trajectory tracking accuracy of conti–nuum robots, including Neural Networks (NNs) control, adaptive control, fuzzy logic control, nonlinear model predictive control, etc. In General, these techniques are suitable for robotic systems with nonlinear, complex, and unknown models under uncertainties and distur–bances.

In literature, neural network techniques have been used for tracking the trajectory of some continuum robots, using both kinematic and dynamic models, as in [19-21]. In [19], the authors applied the NN technique to control the end-tip of a CBHA by tracking the trajectory without physical interactions with the envi–ronment. In [20], the authors have presented a controller designed for continuum robots utilizing a neural network feed-forward component to compensate for the dynamic uncertainties. Furthermore, a neural network-based tracking controller was presented for a wide range of continuum manipulators [21]. However, this tech–nique suffers from local minima issues, often poor solutions to be used in the training phase to solve the problem. Besides, the excellent performance is mainly related to large-size regressors [22].

Some researchers have been using fuzzy logic control. For instance, in [23], a fuzzy logic controller based on the kinematic model is proposed for auto–nomous execution of end-effector trajectory tracking tasks for a TDCR. In contrast, in [24], a fuzzy logic-based static feedback controller is developed for a single bending section of a TDCR. Furthermore, a fuzzy logic methodology was proposed in [25] to design a nonlinear controller to regulate the end-effector of a continuum manipulator to a constantly desired position, and an intelligent controller based on Fuzzy Reinforcement Learning (FRL) was proposed for the trajectory tracking of a TDCR in [26]. The Taguchi method and evolu–tionary genetic algorithm (GA) tuned the proposed FRL-based control parameters to provide faster con–vergence to the Nash Equilibrium. Even though the fuzzy logic control technique has many advantages,

particularly its robustness to system uncertainty, it requires a significant coding effort.

Other researchers have employed adaptive control schemes [22, 27]. The adaptive neural networks scheme [22] and adaptive support vector regressor controller [27] have been made on a continuum manipulator, namely Compact Bionic Handling Arm (CBHA), in which both controllers are applied to the kinematic models. Furthermore, an adaptive model predictive control is proposed to improve the dynamic performance and eliminate the steady-state error of a soft continuum robot [28]. However, when there are tight constraints to be satisfied, the Model-based Predictive Control (MbPC) algorithm is more suitable and can be a promising alternative for continuum robots control. For instance, a Nonlinear Model Predictive Control (NMPC) scheme is proposed in [29] to control the growth of vine-like growing robots using the kinematic model. In [30], a Nonlinear Evolutionary Model Predic–tive Control (NEMPC) is used to control the pneumatically actuated continuum robot in which its dynamic model is approximated using a Deep Neural Net–work (DNN). In [31], a Model Predictive Control (MPC) has been developed for the autonomous steering of Concentric Tube Robots (CTRs). In the same context, we intend to apply the Nonlinear Model Predictive Control (NMPC) scheme based on the Particle Swarm Optimization (PSO) algorithm to control a class of continuum robots, namely Cable-Driven Continuum Robot (CDCR), using both kinematic and dynamic models.

The paper includes the kinematic and dynamic modeling of a class of continuum robots, namely Cable-Driven Continuum Robot (CDCR), in the planar projection. Then, based on the developed models, a Nonlinear Model Predictive Control (NMPC) scheme is proposed to control the tip of a planar CDCR consisting of a two bending-section. Nevertheless, the main draw–back of applying the NMPC schemes is related to the computational burden associated with optimization algorithms that must be solved in each sampling period. In this paper, the Particle Swarm Optimization (PSO) algorithm is used as a solution to the optimization problem arising in the MBPC, due to its simplicity and fast convergence. Thus, the NMPC-PSO controller, based on the kinematic and dynamic models, enables the states of the planar CDCR to track a desired reference trajectory in free Cartesian space.

The outline of this paper proceeds as follows: Section 2 summarizes the kinematics modeling of a cable-driven continuum robot in the planar projection. Section 3 presents the dynamic model development. Section 4 focuses on developing the proposed Nonlinear Model of Predictive Control and the optimizer method, namely Particle Swarm Optimization. Section 5 presents the simulation results used to illustrate the proposed controllers' effectiveness and performance. Some conc–luding remarks and prospects are drawn in Section 6.

2. KINEMATIC MODELS

The schematic structure of the famous hard class of continuum robots with three cable actuators per bending section, namely the Cable-Driven Continuum Robot

(CDCR), is depicted in Figure 1. It is essential to highlight that by serially connecting the bending sections, a CDCR with multiple bending sections can be constructed, i.e., with n bending sections and $3 \times n$ cable actuators. Hence, each bending section has an elastic core (usually called backbone) along which are rigidly mounted m rigid spacer disks. The bending and orientation motion of each bending section is made by the deflection of the elastic core by applying suitable tension on one or two cables at the same time. In the following analysis, only the bending motion is considered, particularly in the planar projection.
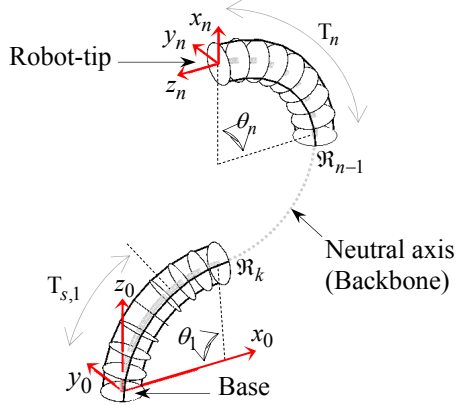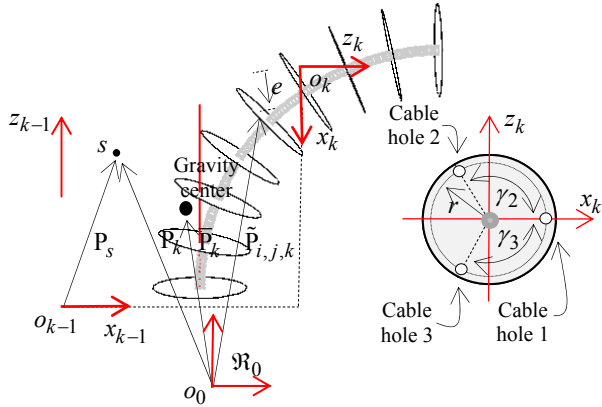

Figure 1. CDCR schematics

Figure 2. Single bending-section schematics

2.1 Forward Kinematics

It is of paramount importance to note that in order to establish the dynamic model, kinematic models, inc–luding local and global positions and velocities, will be first derived. However, the Constant Curvature Kine–matic Approach (CCKA) [7] is generally used in modeling among the approaches proposed to handle the forward kinematics of continuum robots.

Based on this kinematic analysis, the homogeneous transformation matrix T_s that contains the position vector P_s and the rotation matrix R_s of any frame attached at s, with $s \in [0, l_k]$, on the backbone of the bending-section k in the local reference frame $\Re_{k-1}$ $(o_{k-1}, x_{k-1}, y_{k-1}, z_{k-1})$ can be calculated as follows:

$$T_s = \begin{bmatrix} R_s & P_s \\ 0^T & 1 \end{bmatrix}, \qquad (1)$$

In accordance with [7], the components P_s and R_s of T_s are given as the following:

$$P_s = \frac{l_k}{\theta_k}\left[1-c\left(\frac{s\theta_k}{l_k}\right) \quad 0 \quad s\left(\frac{s\theta_k}{l_k}\right)\right]^T, \qquad (2)$$

$$R_s = \begin{bmatrix} c\left(\dfrac{s\theta_k}{l_k}\right) & 0 & s\left(\dfrac{s\theta_k}{l_k}\right) \\ 0 & 1 & 0 \\ -s\left(\dfrac{s\theta_k}{l_k}\right) & 0 & c\left(\dfrac{s\theta_k}{l_k}\right) \end{bmatrix}, \qquad (3)$$

where s is the curvilinear parameter that represents the length from the origin of the reference frame $\Re_{k-1}$ to the specified point s, and the abbreviations $c(\cdot)$ and $s(\cdot)$ mean respectively $\cos(\cdot)$ and $\sin(\cdot)$.

More generally, the homogeneous transformation matrix T_k defining any frame attached at s to the backbone of the bending-section k, with $k = 1,2,\ldots,n$, the global reference frame $\Re_0(o_0, x_0, y_0, z_0)$ can be calculated as follows:

$$T_k(\theta) = \begin{bmatrix} R_k(\theta) & P_k(\theta) \\ 0^T & 1 \end{bmatrix} = \prod_{\xi=1}^{k-1} T_\xi . T_s . \qquad (4)$$

where $\theta = \begin{bmatrix} \theta_1 & \ldots & \theta_k \end{bmatrix}^T$ is the vector of the bending angles that will be used as generalized coordinates in the following section.

For further use, since each backbone k is considered to have a uniform mass distribution, the position vector of its gravity center $\overline{P}_k$ relative to the global reference frame $\Re_0$ can be calculated as follows [10]:

$$\overline{P}_k = P_{k-1} + \frac{\int_0^{l_k} P_s . ds}{l_k} = P_{k-1} + \begin{cases} \dfrac{l_k}{\theta_k^2}(\theta_k - s(\theta_k)). \\ 0. \\ \dfrac{l_k}{\theta_k^2}c(\theta_k). \end{cases} \qquad (5)$$

Furthermore, the position vector of the cable holes $\tilde{P}_{i,j,k}$ on the disk j for the bending-section k relative to the global reference frame $\Re_0$ can be obtained as follows:

$$\tilde{P}_{i,j,k} = T_{j,k} . r_i , \qquad (6)$$

where $T_{j,k}$ is calculated at $s = jl_k/m$, with $j = 1,2,\ldots,m$ using equation (4), and r_i is the position vector of the routing holes on the disk in its local reference frame that can be expressed as follows:

$$r_i = r\begin{bmatrix} c(\gamma_i) & s(\gamma_i) & 0 & 1 \end{bmatrix}^T, \qquad (7)$$

where r is the radial distance from the center of the disk to the routing holes, and γ_i is the arrangement angle of the cable holes on the disk given as follows:

$$\gamma_i = \begin{cases} 0, & i = 1 \\ 2\pi/3, & i = 2 \\ -2\pi/3, & i = 3 \end{cases} \qquad (8)$$

2.2 Differential kinematics

The linear velocity $\dot{P}_k$ at any point s can be obtained by direct differentiation with respect to the time of the vector position P_k, while the angular velocity ω_k can be expressed as follows [11]:

$$\omega_k = \omega_{k-1} + R_{k-1} . \omega_s . \qquad (9)$$

with

$$\omega_s = \hat{t}_s . \dot{t}_s , \qquad (10)$$

where t_s is the third vector column of the rotation matrix R_s, $\hat{t}_s$ is the associated skew matrix of the vector t_s and $(\cdot)$ means the differentiation with respect to time.

3. DYNAMIC MODEL

In order to derive a dynamic model of multisection CDCR using the Lagrange method for general coordi–nates θ, the kinetic energy, the potential energy, and the corresponding generalized forces will be derived first.

$$\frac{d}{dt}\frac{\partial T}{\partial \dot{\theta}} - \frac{\partial T}{\partial \theta} + \frac{\partial U}{\partial \theta} = Q . \qquad (11)$$

where T, U and Q are kinetic energy, gravitational energy, and generalized forces, respectively.

3.1 Kinetic energy

The kinetic energy, including translational and rotati–onal kinetic energy, of a multisection CDCR concerning the global reference frame $\Re_0$ can be expressed as fol–lows:

$$T = T_{trans} + T_{rot} . \qquad (12)$$

with

$$T_{trans} = T^b_{trans} + T^d_{trans} . \qquad (13)$$

$$T_{rot} = T^b_{rot} + T^d_{rot} . \qquad (14)$$

where T^b_{trans}, T^d_{trans}, T^b_{rot} and T^d_{rot} are the translati–onal and rotational kinetic energy of the backbone and the disks, respectively.

As mentioned above, the distribution mass of each backbone is assumed to be uniform, and the disks are mounted on the elastic core at an equal distance and have the same mass. Therefore, the translational kinetic energy of the backbones and disks can be calculated respectively as follows:

$$T^b_{trans} = \frac{1}{2}\sum_{k=1}^{n}\int_0^{l_k} \dot{P}_k^{\mathrm{T}} . m_k^b . \dot{P}_k \, ds , \qquad (15)$$

$$T^d_{trans} = \frac{1}{2}\sum_{k=1}^{n}\sum_{j=1}^{m} \dot{P}_{j,k}^{\mathrm{T}} . m_{j,k}^d . \dot{P}_{j,k} , \qquad (16)$$

where m_k^b and $m_{j,k}^d$ are the backbone and disk mass, respectively.

Similarly, the rotational kinetic energy of the back–bone and the disks can be calculated respectively as follows:

$$T^b_{rot} = \frac{1}{2}\sum_{k=1}^{n}\int_0^{l_k} \omega_k^{\mathrm{T}} . I_k^b . \omega_k \, ds , \qquad (17)$$

$$T^d_{rot} = \frac{1}{2}\sum_{k=1}^{n}\sum_{j=1}^{m} \omega_{j,k}^{\mathrm{T}} . I_{j,k}^d . \omega_{j,k} , \qquad (18)$$

where I_k^b and $I_{j,k}^d$ are the moment of inertia of the backbone k and the disk (j,k), respectively. Equation (18) $\omega_{j,k}$ is calculated at $s = jl_k/m$, with $j = 1, 2, ..., m$, using equation (9).

3.2 Potential energy

The total potential energy of a multi-section CDCR consists of two parts: gravitational potential energy and elastic potential energy.

$$V = V_{gr} + V_{els} . \qquad (19)$$

The backbones and disks are subject to gravity. Therefore, their total gravitational potential energy can be obtained as the following:

$$V_{gr} = V_d + V_b . \qquad (20)$$

with

$$V_d = \sum_{k=1}^{n}\sum_{j=1}^{m} G . m_{j,k}^d . P_{j,k} , \qquad (21)$$

with

$$G = g\begin{bmatrix} 0 & 0 & -1 \end{bmatrix}^{\mathrm{T}} , \qquad (22)$$

where g is the gravitational constant.

$$V_b = \sum_{k=1}^{n} G . m_k^b . \bar{P}_k , \qquad (23)$$

The total elastic potential energy of all backbones can be calculated as follows [6]:

$$V_{els} = \sum_{k=1}^{n} \frac{E.I_k^b}{2l_k} \theta_k^2 , \qquad (24)$$

where E is the Young's modulus.

3.3 Generalized forces

The generalized force applied to the robot consists of actuation forces, external forces, and frictional forces. However, as each bending section is curved in a circular arc shape; therefore, the external forces and the frictional forces coming from the contact between the cables and the routing holes will not be taken into

account in this case. However, the cables are attached to the end disk of each bending section; the generalized force exerted on the end disk of each bending section by cable i can be calculated as the following:

$$Q = \sum_{i=1}^{3} \left(\frac{\partial \tilde{P}_{i,m,k}}{\partial \theta} \right)^{\text{T}} \cdot f_{i,k} \cdot \frac{\tilde{P}_{i,m-1,k} - \tilde{P}_{i,m,k}}{\left\| \tilde{P}_{i,m-1,k} - \tilde{P}_{i,m,k} \right\|}, \quad (25)$$

where $f_{i,k}$ is the magnitude of the actuation force of cable i exerted on the enddisk m of the bending-section k.

3.4 Resulting models of a two bending-section CDCR

It is noteworthy that detailed kinematic and dynamic models are needed to implement the controller. The resulting Cartesian kinematic models of a two bending-section CDCR in the planar projection are presented in Appendix A. However, regarding the dynamic model of the considered robot, given that the elements involved in the dynamic model have very long and complex expressions; therefore, it will be presented in the general form as follows:

$$M(\theta)\ddot{\theta} + C(\theta,\dot{\theta}) + K(\theta) = D(\theta)Q. \quad (26)$$

The state variables described in equation (27) are used to present the dynamical model in the state space representation. Then, the fourth-order Runge-Kutta method is used as a numerical solution.

$$\begin{cases} S_1(t) = \theta_1(t), & S_2(t) = \dot{S}_1(t), \\ S_3(t) = \theta_2(t), & S_4(t) = \dot{S}_3(t), \end{cases} \quad (27)$$

Thereby, the dynamic model can be written in the general form as follows:

$$\dot{S}(t) = F(S,t) + H(S,t) \cdot u(t). \quad (28)$$

where $S(t)$ represents the state variable vector, $F(S,t)$ and $H(S,t)$ are nonlinear functions, and u(t) represents the command vector.

4. CONTROLLER DESIGN

The basic idea of Nonlinear Predictive Control consists in calculating, at each sampling time over the prediction horizon, a control sequence aimed at minimizing an appropriate quadratic cost function taking into account the physical and environmental constraints. Hence, this section summarizes the NMPC strategy and the applied optimizer method, namely Particle Swarm Optimization (PSO).

4.1 NMPC formulation

Model predictive control has become an attractive feedback strategy, predominantly linear processes. However, many robotic systems, particularly continuum robots, are governed by nonlinear and complex models, whether kinematic or dynamic and generally have inaccuracies in modeling approaches. These factors motivate the use of Nonlinear Model Predictive Control (NMPC) to describe such a system's highly nonlinear

processes and nonlinear models. On the other hand, The computation burden associated with the optimization problem of the NMPC is persisting as a challenge for the application of the NMPC schemes to control systems that present fast dynamics. Various algorithms have been proposed to solve the optimization problem of the NMPC. Sequential Quadratic Programming (SQP) is the most efficient algorithm for solving the optimization problem of the NMPC, but it is time-consuming. Other algorithms have been proposed to solve this problem in a reasonable computation time, such as a nonlinear sum of squares [32] and the multiple shooting method [33], but these remain quite difficult to code. In [34], the control law is computed offline, and the controller is implemented online as a lookup table. In [35], a varying-parameter one-layer projection neural network is used to solve a quadratic programming optimization problem of the NMPC to control a mobile medical robot.

Nowadays, metaheuristic optimization algorithms effectively find reasonable solutions for complicated real-life problems. In [36], Particle Swarm Optimization (PSO) and Gravitational Search Algorithm (GSA) have been applied to resolve the optimization problem of the NMPC to control a wheeled mobile robot. Ant Colony Optimization algorithm(ACO) was applied to solve the MPC optimization problem to control the torque of a three-phase induction motor [37]. This paper uses the PSO algorithm to solve the arising optimization problem in NMPC due to its simplicity and fast convergence[38].

Designing the control law aims to ensure that the robot tracks the reference trajectory without error. Thus, it x_τ is the state space and u_τ is the control signal. The nonlinear state-space model representing the motion of any robotic system may be described as follows:

$$\begin{cases} x_{\tau+1} = F(x_\tau, u_\tau), \\ \text{s.t.} \\ u_\tau \in U, \quad x_\tau \in X. \end{cases} \quad (29)$$

where F is a continuous mapping with $F(0,0) = 0$. U and X are the set of feasible input and state values, respectively.

It should be stressed that the optimization problem to be solved by the NMPC can be formulated as follows:

$$\min_{U} J_N(x, u, \tau), \quad (30)$$

where the cost function J to be minimized over the optimization horizon N is expressed as the following:

$$J_N(x, u, \tau) = \Psi(x_{\tau+N}) + \sum_{A=\tau}^{\tau+N-1} (x_d - x_a)^{\text{T}} (x_d - x_a). \quad (31)$$

where N is the optimization horizon, $\Psi(x_{\tau+N})$ the weight on the final state space, and x_d, x_a the desired and the actual state, respectively.

In the NMPC strategy, the problem is solved to obtain the optimal control sequences $u = [u_\tau \ldots u_{\tau+N+1}]$ over a finite prediction horizon, but only the first control

sequence is applied to the robot. To sum it up, the prob–lem is to find the control sequences defined by θ_k, with $k = 1,2,…,n$, that allows the robot to track a given reference trajectory defined in the task space. The block diagram of the proposed NMPC-POS is shown in figure 3.
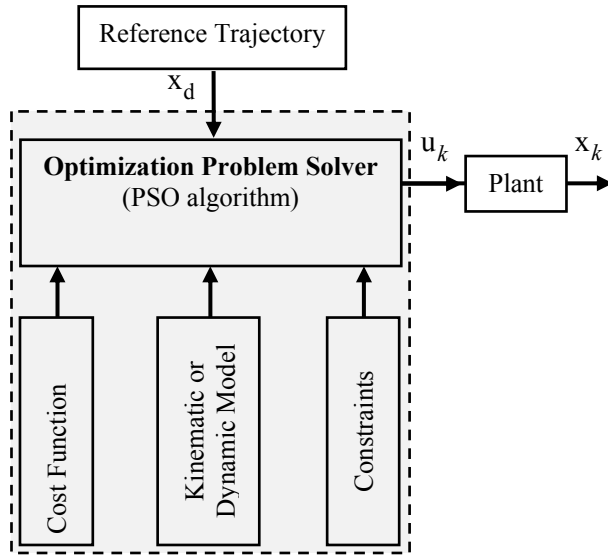

Figure 3. Block diagram of the proposed MPC-PSO

4.2 Optimization method

It is crucial to accentuate that, in this study, the Particle Swarm Optimization (PSO) method is used to solve the arising optimization problem in NMPC, thanks to its simplicity and fast convergence.

In 1995, Kennedy and Eberhart introduced a new metaheuristic method called Particle Swarm Optimi–zation [39], which is an evolutionary optimization technique based on the social behavior of bird flocks in search of food. In a PSO method, each possible solution is called a particle, and the population is the swarm. Basically, the initial phase consists of randomly gene–rating the population in the search space, where each particle p has its own position x_p^τ and velocity v_p^τ. In each iteration τ, the position of each particle is updated as a function of the local best position P_{pbest}^τ and the global best position P_{gbest}^τ. Therefore, the position and velocity of each particle are updated according to the following equations:

$$v_p^{\tau+1} = v_p^\tau + \sigma_1\rho_1\left(P_{pbest}^\tau - x_p^\tau\right) + \sigma_2\rho_2\left(P_{gbest}^\tau - x_p^\tau\right). \quad (32)$$

$$x_p^{\tau+1} = x_p^\tau + v_p^{\tau+1}. \quad (33)$$

where σ_1 and σ_2 are positive constants; ρ_1 and ρ_1 are two random variables with a uniform distribution between 0 and 1.

Although the PSO method is a faster convergence algorithm than other optimization algorithms and is used to construct the control scheme [38, 40-41], in contrast to those benefits, the common drawback of optimization methods is the early convergence of the solution towards the local minima. A swarm regene–ration technique was added to the PSO algorithm [42].

5. SIMULATION RESULTS

In this section, the effectiveness and performance, in terms of tracking accuracy and computation time, of the proposed NMPC-PSO controller based on the developed kinematic and dynamic models are examined and compared. To achieve this purpose, two simulation examples are performed. The first example shows the convergence of the two controllers for a desired robot's end-point. In contrast, the second one is proposed to implement the controller on a CDCR for tracking a trajectory in a free Cartesian environment for both kinematic and dynamic models. A two bending-section CDCR is simulated for all case studies, inside its workspace, with the estimated geometric and material detailed in Table 1. The parameters of the PSO method are given in Table 2. Eventually, the simulations are conducted on MATLAB software using Intel (R) Core (TM) i3-2310M CPU at 2.10 GHz and 4Go RAM.

Table 1. Geometrics and material of the simulated CDCR

j	5	$r_{j,k}^d$	20 mm
k	2	r_k^b	2.5 mm
m_k^b	0.032 kg	r	19 mm
$m_{j,k}^b$	0.010 kg	E	2.1 GPa
l_k	300 mm	g	9.81 m/s²

Table 2. PSO parameters

Swarm size	Inertia	iterations	Correction factor
100	1.25	50	1.02

4.3 Set-point Stabilization

It is worth noting that this simulation aims to highlight the performance of the proposed NMPC-PSO with the kinematic and dynamic models during the set-point stabilization simulation, which does not involve time as a constraint. Figures 4 and 5 show the perfect tracking of two controllers to reach the goal predefined as [100,0,400] (mm), where the robot's simulation models begin from the initial position as [50,0,500] (mm).
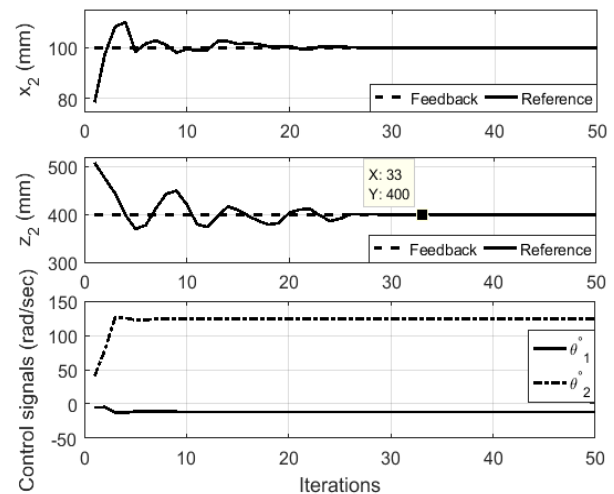

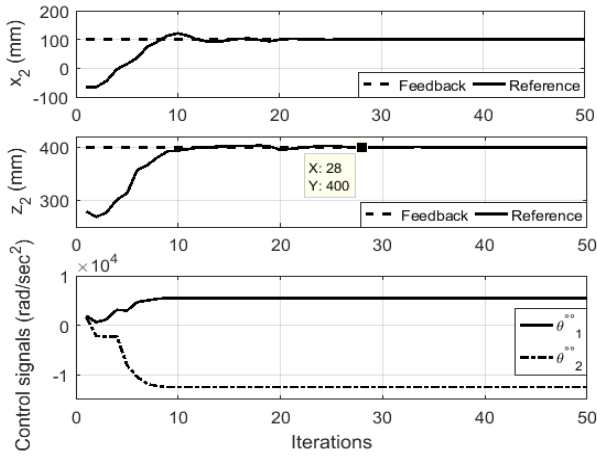**Figure 4. Results of set-point simulation to evaluate the stabilization of the controller with the kinematic model**

Figure 5. Results of set-point simulation to evaluate the stabilization of the controller with the dynamic model

From these Figures, it is clear that NMPC-PSO with the dynamic model is more stable than that with the kinematic model since the controller stabilizes the robot's end-tip at the goal after 28 iterations against 33 iterations for the kinematic controller. In addition to that, the NMPC-PSO joined with the dynamic model eliminates the oscillations present in the state variables x and z. In contrast, the controller with the kinematic model took less computational time (5.9 msec) that joined with the dynamic model (9.16 msec).

4.4 Trajectory tracking in a free Cartesian environment

In the second simulation example, the NMPC-PSO based on the kinematic and dynamic models is evalu–ated against tracking a circular-shaped trajectory in a free Cartesian environment. The reference trajectory is described in Equation (34). The control sampling time is equal to 0.01 seconds for the total duration of movement as 10 sec.

$$\mathbf{x}_d = \left\{ 50\sin\left(\frac{\pi t}{5}\right) \quad 550 + 50\cos\left(\frac{\pi t}{5}\right) \right\}^T, \quad (34)$$

The obtained simulation results of both controllers' trajectory tracking and control signals are presented in Figures 6, 7, 8, and 9.
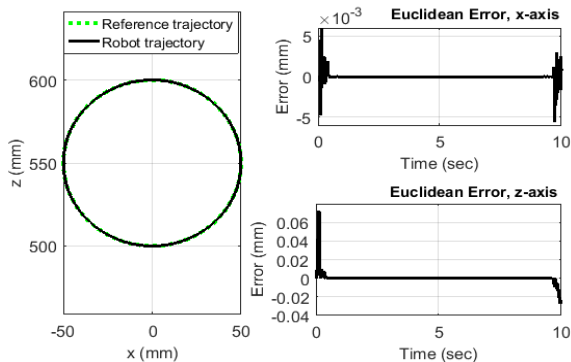

Figure 6. Actual and reference trajectories and the Euclidean errors between them using the kinematic model

From Figures 6 and 7, it is readily apparent that the curves are almost superposed where the mean Euclidean

errors between the actual and reference trajectory along x-axis and z-axis respectively are smaller than $7 \cdot 10^{-5}$ (mm) and $3 \cdot 10^{-4}$ (mm) for the controller joined with the kinematic model, and smaller than $2 \cdot 10^{-5}$ (mm) and $6 \cdot 10^{-6}$ (mm) for the dynamic controller. The presented results show good trajectory tracking for both cont–rollers.
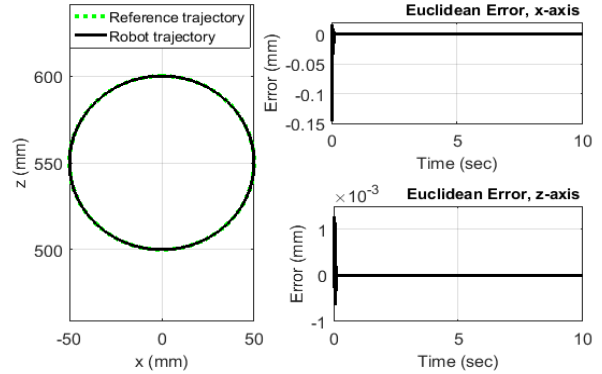

Figure 7. Actual and reference trajectories and the Euclidean errors between them using the dynamic model

To clarify more about the oscillations which appear when using the NMPC-PSO joined with the kinematic model, Figure 8 highlights the oscillations that appear in the angular velocity versus those calculated from the control signals of the controller joined with the dynamic model (see, Figure 9).
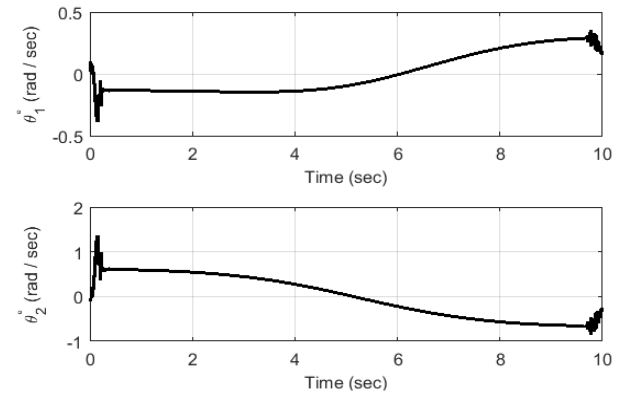

Figure 8. The angular velocity with the kinematic NMPC-PSO
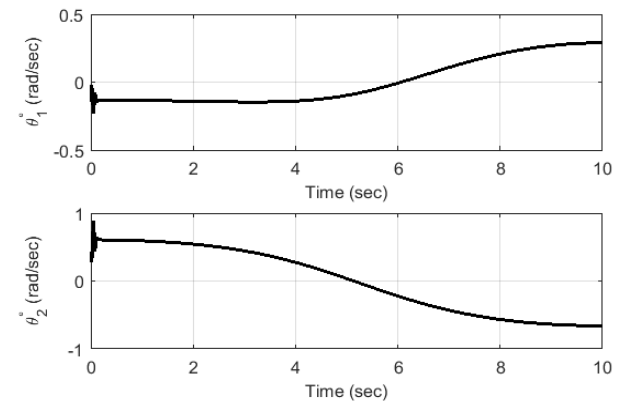

Figure 9. The angular velocity with the dynamic NMPC-PSO

The two controllers' required computation times to track the circular-shaped trajectory are presented in figures 10 and 11, respectively. Figure 10 shows the

relatively low computation times of NMPC-PSO based on the kinematic model compared to that joined with the dynamic model, where the mean computational time for the two controllers is less than 5.5 msec and 8.89 msec, respectively. So, these results are very encouraging for real-time applications of the two controllers. However, the computation time of the optimization methods depends on the number of variables to be optimized, i.e., to be found. So, as the robot's bending-sections increase, the computation time will increase proportionally.
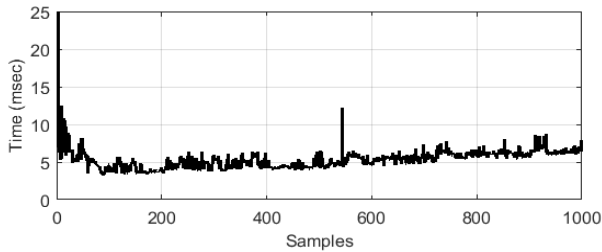

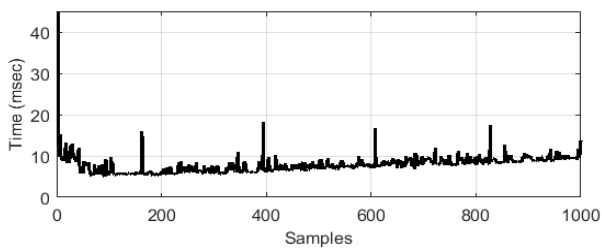**Figure 10. Computation times for the kinematic NMPC-PSO**

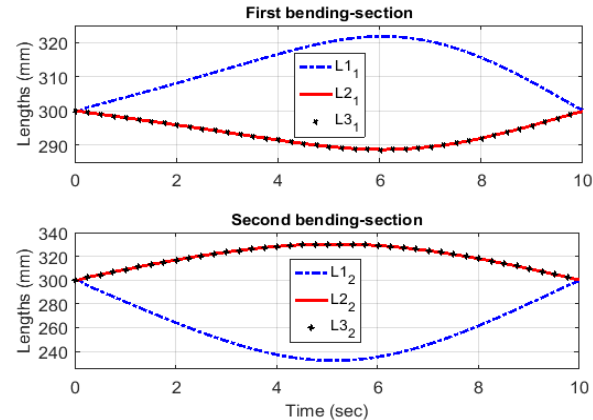**Figure 11. Computation times for the dynamic NMPC-PSO**

Figure 12. Evaluation of cable lengths for the kinematic NMPC-PSO

Moreover, the temporal evolutions of the cable lengths necessary to track the circular-shaped trajectory, which is calculated using the results obtained from the NMPC-PSO based on the kinematic model, are shown in Figure 12. Similarly, the temporal evolutions of the required tensions applied on the cables for tracking the desired trajectory, calculated using the results obtained from the NMPC-PSO based on the dynamic model, are shown in Figure 13.

To sum up, the analysis of the previously presented simulation results confirms the possibility of applying successfully the proposed NMPC-PSO, based on the kinematic and dynamic models, for trajectory tracking for a class of continuum robots, namely Cable-Driven Continuum Robot (CDCR).
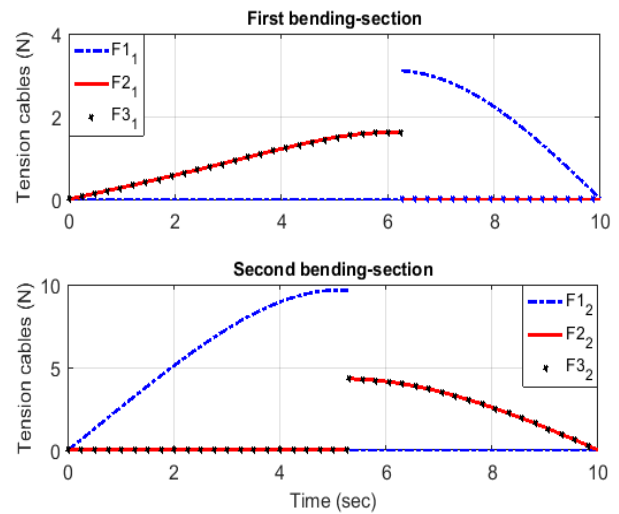

Figure 13. Evaluation of tensions applied on the cables for the dynamic NMPC-PSO

For comparison, the proposed NMPC-PSO based on the dynamic model has achieved a good performance in trajectory tracking accuracy, smoothness in control signals, and absence of oscillations in the state variables compared to the kinematic one. In contrast, the proposed NMPC-PSO based on the kinematic model took less computation time and was easier in formulation than the dynamic one.

Generally, continuum robots have different characteristics and are not controlled with the same inputs. Therefore, it is difficult to directly compare the proposed control techniques based only on the obtained results. Table 3 lists some contributions in continuum robot control techniques, in which trajectory tracking accuracy results were displayed. By analyzing the results of these contributions, it can be seen that the proposed NMPC-PSO scheme achieves the best performance in terms of trajectory tracking accuracy. However, it should be noted that there are other factors affecting the performance of the controller, such as (1) the used mathematical model (kinematic or dynamic model), (2) the model's complexity, (3) the number of bending-section of the robot, and (4) the robot control space (2- or 3-dimensional space).

In a nutshell, it can be said that the proposed NMPC-PSO scheme showed a real ability for real-time imple-mentation and high accuracy of trajectory tracking, making it a promising alternative controller for continuum robots and especially for the cable-driven continuum robot class.

Table 3. Some contributions in the control of continuum robots

Robot characteristics	Control techniques	Trajectory tracking control
CDCR: Continuous shape, rigid structure, two bending sections, controlled by cables.	NMPC-PSO scheme: Proposed scheme.	Accuracy: $< 3 \cdot 10^{-4}$ mm; Validation: Simulation of a planar robot in a free environment.

CBHA: Continuous shape, soft structure, two bending sections, pneumatic actuation.	Nonadaptive neural network controller [22].	Accuracy: 15 mm; Validation: Simulation and real-time experiments.
	Adaptive neural network controller [22].	Accuracy: 5 mm; Validation: Simulation and real-time experiments.
	Nonadaptive support vector regressor controller [27].	Accuracy: 11 mm; Validation: Simulation and real-time experiments.
	Adaptive support vector regressor controller [27].	Accuracy: 5 mm; Validation: Simulation and real-time experiments.
Large-Scale Soft Robot.	Model reference predictive adaptive control [29].	Accuracy: $9 \cdot 10^{-4}$ mm; Validation: Simulation.
TDCR: Continuous shape, rigid structure, controlled by wire cables.	Fuzzy-logic-based static feedback controller [24].	Accuracy: 0. 5 mm Validation: real-time experiment.
	Fuzzy-Model-Based Approach [23].	Accuracy: 0.7165 mm; Validation: real-time experiment.
Vine-like growing robot: Continuous shape, pneumatic actuator muscles, controlled by air pressure.	NMPC-based growth control [29].	Not available.
CTR: Continuous shape, soft structure, actuated by mecha–nisms external to the backbone.	Nonlinear Model Predictive Control [31].	accuracy: $< 5 \cdot 10^{-4}$ m; Validation: Simulation and real-time experiments.

6. CONCLUSION

This paper proposes a Nonlinear Model Predictive Control (NMPC) scheme to solve the trajectory tracking for a class of continuum robots, namely Cable-Driven Continuum Robot (CDCR). The Particle Swarm Opti–mization (PSO) algorithm was used to solve the optimization problem arising in the NMPC. This metaheuristic method has strong advantages compared to other algorithms, such as its simplicity to code and its fast convergence that provides a low computation time. First, the kinematic and dynamic models of two-dimensional CDCR with two bending sections are developed. The dynamic model is derived using the Euler-Lagrange method based on kinematic equations of inextensible bending-section and the Constant Curva–ture Kinematic Approach (CCKA). Based on the developed kinematic and dynamic models of the CDCR, an NMPC-PSO scheme was proposed to solve the trajectory tracking problem. For the two controllers, joined with the kinematic and dynamic models, the simulation was performed on set-point stabilization and trajectory tracking in MATLAB software. Because of the obtained simulation results, the two proposed schemes have succeeded in controlling the tip of the considered CDCR, in a free Cartesian environment, in real-time and with high accuracy. The obtained computation times and quality of the solution in terms of the trajectory tracking accuracy show that NMPC-PSO, based on the kinematic and dynamic models, is a feasible alternative for real-time applications.

In terms of dynamic control versus kinematic control, the obtained results show the effectiveness of the NMPC-PSO based on the dynamic model to track the desired trajectory with high accuracy, zero oscillations, and smoothness in control signals. In contrast, the NMPC-PSO based on the kinematic model is easier to implement and takes lower computational time compared to when it is based on the dynamic one.

In comparison with works [22-23, 31] in terms of trajectory tracking accuracy, it is observed that the proposed NMPC-PSO scheme, based on both kinematic and dynamic models, can track the desired trajectory in real-time with high accuracy. The analysis of the available contributions in the control of continuum robots provides an additional argument to support the idea that the proposed NMPC-PSO schemes can improve the performance of these continuum robots, especially those of the considered class, namely Cable-Driven Continuum Robots (CDCRs) for trajectory tracking problem.

As a perspective, we intend to extend the proposed NMPC-PSO scheme to a continuum robot in 3D space configurations and consider obstacle avoidance during trajectory tracking.

APPENDIX A

The developments of kinematic and differential kinematic models used in this paper are presented, respectively, as follows:

$$\mathrm{x} = \begin{cases} x_2 = \dfrac{l}{\theta_1\theta_2}\big(\theta_2 + \theta_1 \mathrm{c}(\theta_1) - \theta_2 \mathrm{c}(\theta_1) - \theta_1 \mathrm{c}(\theta_1 + \theta_2)\big), \\ z_2 = \dfrac{l}{\theta_1\theta_2}\big(\theta_2 \mathrm{s}(\theta_1) - \theta_1 \mathrm{s}(\theta_1) + \theta_1 \mathrm{c}(\theta_1 + \theta_2)\big), \end{cases} \quad (36)$$

$$\dot{\mathrm{x}} = \begin{bmatrix} J_{11} & J_{12} \\ J_{21} & J_{22} \end{bmatrix} \begin{Bmatrix} \dot{\theta}_1 \\ \dot{\theta}_2 \end{Bmatrix} \quad (37)$$

with

$$J_{11} = \dfrac{l}{\theta_1^2\theta_2}\begin{pmatrix} \theta_2 \mathrm{c}(\theta_1) - \theta_2 - \theta_1^2 \mathrm{s}(\theta_1) + ... \\ \theta_1^2 \mathrm{s}(\theta_1 - \theta_2) + \theta_1\theta_2 \mathrm{s}(\theta_1) \end{pmatrix}. \quad (38)$$

$$J_{12} = \frac{-l}{\theta_2^2}\left(c(\theta_1) - c(\theta_1 - \theta_2) + \theta_2 s(\theta_1 - \theta_2)\right). \quad (39)$$

$$J_{21} = \frac{-l}{\theta_1^2 \theta_2}\left(\begin{array}{c} \theta_2 s(\theta_1) - \theta_1^2 c(\theta_1) + \dots \\ \theta_1^2 c(\theta_1 - \theta_2) - \theta_1 \theta_2 c(\theta_1) \end{array}\right). \quad (40)$$

$$J_{22} = \frac{l}{\theta_2^2}\left(s(\theta_1 - \theta_2) - s(\theta_1) + \theta_2 c(\theta_1 - \theta_2)\right). \quad (41)$$

REFERENCES

[1] Robinson, G. and Davies, J.B.C.: Continuum robots - state of the art, in *Proceedings IEEE International Conference on Robotics and Automation*, Detroit, Michigan, pp. 2849–2854, 1999.

[2] Trivedi, D., Rahn, C.D., Kier, W.M. and Walker, I.D.: Soft robotics: biological inspiration, state of the art, and future research, Applied Bionics and Biomechanics, Vol. 5, No. 3, pp. 99–117, 2008.

[3] Chikhaoui, M.T., Rabenorosoa, K.., Andreff, N.: Kinematics and performance analysis of a novel concentric tube robotic structure with embedded soft micro-actuation, Mech. Mach. Theory, Vol. 104, pp. 234–254, 2016.

[4] Amanov, E., Nguyen, T.D. and Burgner-Kahrs, J.: Tendon-driven continuum robots with extensible sections - A model-based evaluation of path-following motions, Int. J. of Robotics Research, Vol. 40, No. 1, pp. 7–23, 2021.

[5] Falkenhahn, V., Mahl, T., Hildebrandt, A., Hildebrandt, A., Neumann, R. and Sawodny, O.: Dynamic modeling of bellows-actuated continuum robots using the Euler-Lagrange formalism, IEEE Trans. on Robotics, Vol. 31, No. 6, pp. 1483–1496, 2015.

[6] Amouri, A., Zaatri, A. and Mahfoudi, C.: Dynamic modeling of a class of continuum manipulators in fixed orientation, Journal of Intelligent and Robotic Systems, Vol. 91, No. 3-4, pp. 413–424, 2018.

[7] Webster, R.J. and Jones, B.A.: Design and kinematic modeling of constant curvature continuum robots: A review, Int. J. of Robotics Research, Vol. 29, No. 13, pp. 1661–1683, 2010.

[8] He, B., Wang, Z., Li, Q., Xie, H. and Shen, R.: An analytic method for the kinematics and dynamics of a multiple-backbone continuum robot, Int. J. of Advanced Robotic Systems, Vol. 10, pp. 1–13, 2013.

[9] El-Hussieny, H., Jeong, S.G. and Ryu, J.H.: Dynamic modeling of a class of soft growing robots using Euler-Lagrange formalism, in: *Proceedings of SICE Annual Conference, Society of Instrument and Control Engineers*, Hiroshima, Japan, 2019.

[10] Dehghani, M. and Moosavian, S. Ali A.: Dynamics modeling of a continuum robotic arm with a contact point in planar grasp, Journal of Robotics, Vol. 2014, Article ID 308283, 2014.

[11] Rone, W. and Ben-Tzvi, P.: Continuum robot dynamics utilizing the principle of virtual power, IEEE Trans. on Robotics, Vol. 30, No. 1, pp. 275–287, 2014.

[12] Rone, W. and Ben-Tzvi, P.: Mechanics modeling of multi-segment rod-driven continuum robots, Journal of Mechanisms and Robotics, Vol. 6, No. 4, 2014.

[13] Renda, F., Boyer, F., Dias, J. and Seneviratne, L.: Discrete Cosserat approach for multisection soft manipulator dynamics, IEEE Trans. on Robotics, Vol. 34, No. 6, 2018.

[14] Orekhov, A.L. and Simaan, N.: Solving Cosserat rod models viacollocation and the magnus expansion, in: *Proceedings of IEEE/RSJ Int. Conf. Intell Robots Sys*, pp. 8653–8660, 2020,.

[15] Gravagne, A., Rahn, C.D. and Walker, I.D.: Large deflection dynamics and control for planar continuum robots, IEEE/ASME Trans. on Mechatronics, Vol. 8, No. 2, pp. 299–307, 2003.

[16] Grazioso, S., Di Gironimo, G., Siciliano, B.: A geometrically exact model for soft continuum robots: the finite element deformation space formulation, Soft Robot Vol. 6, pp. 790–811, 2019.

[17] Renda, F., Boyer, F., Dias, J. and Seneviratne, L.: Discrete Cosserat approach for multisection soft manipulator dynamics, IEEE Trans. Robotics, Vol. 34, pp. 1518–1533, 2018.

[18] Della Santina, C., Katzschmann, R. K.., Biechi, A. and Rus, D.: Dynamic control of soft robots interacting with the environment, in: *Proceedings of IEEE International Conference on Soft Robotics,* pp. 46–53, 2018.

[19] Melingui, A., Merzouki, R., and Mbede, J.: Compact bionic handling arm control using neural networks, Electron. Lett, Vol. 50, No. 14, pp. 979–981, 2014.

[20] Braganza, D., Dawson, D.M., Walker, I.D., and Nath, N.: A neural network controller for continuum robots. IEEE Trans. on Robotics, Vol. 23, No, 6, pp. 1270–1277, 2007.

[21] Wang, X., Li, Y. and Kwok, K. W..: A survey for machine learning-based control of continuum robots, Frontiers in Robotics and AI, Vol. 8, Article 730330, 2021.

[22] Melingui, A., Lakhal, O., Daachi, B., Mbede, J.B. and Merzouki, R.: Adaptive neural network control of a compact bionic handling arm, IEEE/ASME Trans. on Mechatronics, Vol. 20, No. 6, pp. 2862–2875, 2015).

[23] Qi, P., Liu, C., Ataka, A., Lam, H.K.. and Althoefer, K..: Kinematic control of continuum manipulators using a fuzzy-model-based approach, IEEE Transactions on Industrial Electronics, Vol. 63, No. 8, pp. 5022–5035, 2016.

[24] Ba, W., Dong, X., Mohammad, A., Wang, M., Axinte, D. and Norton, A.: Design and validation of a novel fuzzy-logic-based static feedback controller for tendon-driven continuum robots. IEEE/ASME Trans. on Mechatronics, pp. 3010–3021, 2021.

[25] Qi, P. Liu, C., Zhang, L., Wang, S., Lam, H.K. and Althoefer, K.: Fuzzy logic control of a continuum manipulator for surgical applications, in: *Proceedings of IEEE International Conference on Robotics,* Biomimetics, pp. 413–418, 2014.

[26] Goharimanesh, M., Mehrkish, A. and Janabi-Sharifi, F.: A fuzzy reinforcement learning approach for continuum robot Control, Journal of Intelligent and Robotic Systems, Vol. 100, pp. 809–826, 2020.

[27] Melingui, A., Mvogo Ahanda, J.J., Lakhal, O., Mbede, J.B. and Merzouki, R.: Adaptive algorithms for performance improvement of a class of continuum manipulators. IEEE Transactions on Systems, Man, and Cybernetics: Systems*,* Vol. 48, No. 9, pp. 1531–1541, 2018.

[28] Hyatt, P., Johnson C.C., Killpack M.D.: Model reference predictive adaptive control for large-Scale soft robots, Frontiers in Robotics, AI 7:558027, 2020.

[29] El-Hussieny, H., Hameed, I.A. and Ryu, J.H.: Nonlinear model predictive growth control of a class of plant-inspired soft growing robots. IEEE Access, Vol. 8, pp. 214495–214503, 2020.

[30] Hyatt, P. and Killpack, M.D.: Real-time nonlinear model predictive control of robots using a graphics processing unit, IEEE Robotics and Automation Letters*,* Vol. 5, No. 2, pp. 1468–1475, 2020.

[31] Khadem, M., O'Neill, J., Mitros, Z., Da Cruz, L. and Bergeles, C.: Autonomous steering of concentric tube robots via nonlinear model predictive control, IEEE Transactions on Robotics, Vol. 36, No. 5, 2020.

[32] Franzé, G.: A Nonlinear sum-of-squares model predictive control approach, IEEE Transaction on Automatic Control, Vol. 55, No. 6, pp.1466–1471, 2010

[33] Diehl, M., Bock, H., Leineweber, D. and Schlooder J.: Efficient direct multiple shooting in nonlinear model predictive control, F. Keil, W. ackens, H. Vos, J. Werther (Eds.), Scientific Computing in Chemical Engineering II, Springer, Berlin, 1999.

[34] Bemporad, A., Morari, M., Dua, V. and Pistikopoulos, E. N.: The explicit solution of model predictive control via multiparametric quadratic programming, *in: Proceedings of the American Control Conference*, pp. 872–876, 2000.

[35] Yingbai, H., Junling, F., Karimi, H, R., Mom, F, E. D., Knol, A.,: Nonlinear Model Predictive Control for Mobile Medical Robot Using Neural Optimization, IEEE Transactions on Industrial Electronics , Vol. 68, No. 12, pp. 12636–12645, 2021.

[36] Merabti, H., Belarbi, K., Bouchemal, B.: Nonlinear predictive control of a mobile robot: a solution using metaheuristcs, J. of the Chinese institute of engineers, Vol. 39, No. 3, pp. 282–290, 2016.

[37] Kanungo, B. M., Abhimanyu, S., Rabi, M. N.: Development of MPC-ACO based direct torque controller for induction motor drive, *in:* *Proceedings of 4ᵗʰ Biennia International Conference on Nascent Technologies in Engineering*, pp. 1–7, 2021.

[38] Amouri, A., Mahfoudi, C., Zaatri, A. et al.: A metaheuristic approach to solve inverse kinematics of continuum manipulators, J. of systems and Control Eng, Vol. 231, No. 5, pp. 380–394, 2017.

[39] Kennedy, J. and Eberhart, R.C.: Particle swarm optimization, in: *Proceedings of IEEE international conference on neural networks IV*, pp. 1942–1948, 1995.

[40] Shafiqur, R., Salman A.K. and Luai, M. A.: The effect of acceleration coefficients in particle swarm optimization algorithm with application to wind farm layout design, FME Transactions, Vol. 48, No. 4, pp. 922-930, 2020.

[41] Abe, A.: Nonlinear control technique of a pendulum via cable length manipulation: Application of particle swarm optimization to controller design, FME Transactions, Vol. 41, No. 4, pp. 265–270, 2013.

[42] Ram, R.V., Pathak, P.M. and Junco, S.J.: Inverse kinematics of mobile manipulator using bidirectional particle swarm optimization by manipulator decoupling, Mechanism and Machine Theory, Vol. 131, pp. 385–405, 2019.

NOMENCLATURE

E	Young's modulus.
f	Force.
F	Continuous mapping function.
F	Nonlinear function.
H	Nonlinear function.
i	Cable index, with $i = 1, 2, 3$.
I	Inertia moment.
g	Gravitational constant.
j	Disk index, with $j = 1, 2, ..., m$, numbered from base to tip of the bending section.
J	Cost function.
k	Bending-section index, with $k = 1, 2, ..., n$, numbered from base to tip of the robot.
l_k	Length of the bending section k.
m	Disks number.
m	Mass.
n	Bending-sections number.
N	Optimization horizon.
p	Particle.
P	Position vector at point s on the backbone.
$\overline{P}$	The position vector of the gravity center.
$\tilde{P}$	The position vector of the cable hole.
P_{pbest}	Local best position.
P_{gbest}	Global best position.
Q	Generalized force.
r	Distance from the center of the disk to the routing hole.
R	Rotation matrix.
$r_{j,k}^d$	Radius of disk

r_k^b	Radius of backbone
s	Curvilinear parameter.
S	State variable vector
t	Time.
t	Third vector column of R .
T	Homogeneous transformation matrix.
T	Kinetic energy.
U	Set of feasible input.
u	Control signal.
v	Particle velocity.
V	Potential energy.
x	Particle position.
x	State-space.
X	State values.

Greek symbols

ω	Angular velocity.
τ	Iteration.
θ	Bending angles vector, with $\theta = [\theta_1 \ ... \ \theta_n]^{\mathrm{T}}$.
γ_i	The angle of arrangement of cables in a rotation distance of 120 degrees.
ρ_1, ρ_2	Random variables.
$\eta_{j-1,j}$	The contact angle between the direction of cable tensions
μ	Coefficient of friction.
σ	Represents the direction of frictional force in which their values are either -1 or $+1$.
σ_1, σ_2	Positive constants.
Ψ	Weight on the final state space.
$\Re$	Reference frame.

Abbreviations

a	Actual.
b	Backbone.
c	Cosine.
d	Desired.
d	Disk.
els	Elastic.
gr	Gravitational.
rot	Rotational.
s	Sine.

$trans$	Translational.

ПРЕДИКТИВНА КОНТРОЛА НЕЛИНЕАРНОГ МОДЕЛА КЛАСЕ КОНТИНУАЛНИХ РОБОТА КОРИСТЕЋИ КИНЕМАТСКЕ И ДИНАМИЧКЕ МОДЕЛЕ

А. Амоури, А. Шерфиа, Х. Мерабти, Ј.Л.Д. Лексир

Контролисање континуалних робота са прециз–ношћу је посебно изазован задатак због сложености њихових математичких модела и нетачности у приступима моделирању. Стога је већина напредних контролних шема показала лоше перформансе, посебно у тачности праћења путање. Овај рад представља предложену шему нелинеарног модела предиктивне контроле (НМПК) за решавање праћења путање класе континуалних робота, односно Cable-Driven Continuum Robot (CDCR). Међутим, пошто су НМПК шеме често ограничене рачунским оптерећењем повезаним са алгоритмима оптимизације који се решавају у сваком тренутку узорковања, алгоритам за оптимизацију роја честица (ПСО) се користи за решавање насталог проблема оптимизације НМПК, захваљујући својој једнос–тавности и брзој конвергенцији. Предложена НМПК-ПСО шема је примењена на развијене кине–матичке и динамичке моделе разматраног CDCR-а. На основу кинематичког и динамичког модела, два предложена регулатора су валидирана у односу на нумеричке симулације дводимензионалног CDCR-а са два дела савијања за стабилизацију задате тачке и праћење путање од тачке до тачке. За оба контролера, перформансе тачности праћења и времена израчунавања се анализирају и пореде. Штавише, добијени резултати симулације се пореде са доступним литературним радовима. С обзиром на резултате добијене на разматраном CDCR-у, предложена НМПК-ПСО шема може у реалном времену да прати жељену путању са високом прецизношћу и много краћим временом извршења него друге напредне шеме управљања, што је чини алтернативом за апликације у реалном времену.